

Quaternary compounds Ag_2XYSe_4 (X=Ba, Sr; Y=Sn, Ge) as novel potential thermoelectric materials

A. J. Hong^{*a}, C. L. Yuan^{*a}, and J. -M. Liu^b

^{*}Correspondence and requests for materials should be addressed to A.J.H. (email: 6312886haj@163.com) and C.L.Y. (email: clyuan@jxnu.edu.cn).

^a Jiangxi Key Laboratory of Nanomaterials and Sensors, School of Physics, Communication and Electronics, Jiangxi Normal University, Nanchang 330022, China

^b Laboratory of Solid State Microstructures and Innovation Center of Advanced Microstructures, Nanjing University, Nanjing 210093, China

ABSTRACT: Experimental results have shown that the quaternary compound $\text{Cu}_2\text{ZnSnSe}_4$ is an excellent thermoelectric material. This inspires us to seek the other quaternary compounds with similar chemical formula to $\text{Cu}_2\text{ZnSnSe}_4$ as thermoelectric materials. In this paper, for the first time, we use the full potential method with modified Becke and Johnson potential (mBJ) scheme to explore the electronic structures, mechanical and thermal and thermoelectric properties of p- and n-type Ag_2XYSe_4 (X=Ba, Sr; Y=Sn, Ge). The Fermi-golden rule is employed to calculate the carrier relaxation time related to electrical conductivity, electronic thermal conductivity. It is found suitable band gaps and several carrier pockets account for high electrical conductivities and Seebeck coefficients, strong anharmonic vibrations for acoustic wave lead to low lattice thermal conductivities that are lower than $1.0 \text{ Wm}^{-1}\text{K}^{-1}$ at high temperature. It is predicted that the Ag_2XYSe_4 are a kind of potential thermoelectric materials. The maximum ZT for n-type $\text{Ag}_2\text{SrGeSe}_4$ can reach up to 1.15, and those for p-type $\text{Ag}_2\text{SrSnSe}_4$, $\text{Ag}_2\text{SrGeSe}_4$ and $\text{Ag}_2\text{BaSnSe}_4$ can reach up to 1.04, 1.01 and 1.03 at 900 K, respectively.

I. INTRODUCTION

During the last few decades, with the increasing problems of energy exhaustion and environment pollution, thermoelectric (TE) materials have already aroused people's widespread concern [1,2], due to their special properties of directly converting heat to electricity and vice versa. One can use a dimensionless figure of merit, namely $ZT=S^2\sigma T/\kappa$, to assess the TE materials' conversion efficiency from heat to electricity [3,4]. Herein, S and σ represent the Seebeck coefficient and electrical conductivity, T and κ are the temperature (in unit of Kelvin) and total thermal conductivity composed of electronic κ_e and lattice κ_L contributions. Thus, a good TE material requires high S and σ and low κ . However, this is hard to achieve due to the complex interdependences between S , σ and κ [5]. Recently, it was reported that achieving large band degeneracy [6] or localized resonant state [7] via energy band engineering do improve the TE transport properties in few existing TE materials [8]. Nevertheless, this strategy has great blindness because one is difficult to decide which dopant can induce beneficial change of electronic structure. Another common strategy is to reduce lattice thermal conductivity by low-dimension [9] or solid solution strategies [10,11] and so on, but the reduction of κ_L is often accompanied by reduction of σ . Therefore, seeking new TE materials with medium TE performance and then improving ZT value by tuning the carrier density remains to be a simple and feasible method [12,13].

Recently, quaternary compounds $\text{Cu}_2\text{ZnSn}(\text{S}/\text{Se})_4$ (CZTSSe) are considered as promising photovoltaic absorber material due to high efficiency of about 12.6% [14]. It was reported that the band gaps of pure $\text{Cu}_2\text{ZnSnSe}_4$ (CZTSe) and $\text{Cu}_2\text{ZnSnS}_4$ (CZTS) were about 1.0 [15-17] and 1.5 eV [18,19] close to ideal values of 1.3–1.4 eV for solar cell materials. Band gap is very important parameter for semiconductor application. For TE applications, it is usually agreed that good TE materials should possess narrow band gap < 1.0 eV. For example, star TE materials Bi_2Te_3 , SnSe, PbS, PbSe, PbTe, CoSb₃, NbFeSb, Mg₂Si, Mg₂Ge and Mg₂Sn have band gaps of ~0.15 eV [20], ~0.86 eV [5], ~0.4 eV [21], ~0.29 eV [21], ~0.32 eV [21], ~0.22 eV [22], ~0.51 eV [23], ~0.77 eV [24], ~0.74 eV [25] and ~0.35 eV [26], respectively. By judging from band gaps, instead of CZTS, compound CZTSe seems to be a promising thermoelectric material. In Fact,

previous works have indicated that the ZT of In-doped CZTSe reached up to 0.95 at 850 K [27] and that of modified CZTS was only 0.36 at 700K [28]. Therefore, we tried to replace Cu, Zn and Sn atoms of compound $\text{Cu}_2\text{ZnSnSe}_4$ with Ag, Ba/Sr and Sn/Ge atoms, constructing four new compounds Ag_2XYSe_4 (X=Ba, Sr; Y=Sn, Ge). The structures of $\text{Ag}_2\text{BaGeSe}_4$ and $\text{Ag}_2\text{BaSnSe}_4$ have been experimentally verified to be space group $I222$ (No. 23) [29] and the others were theoretically predicted to be space group $I222$ [30], also. Obviously, Ag_2XYSe_4 structures possess lower symmetry than kesterite $\text{Cu}_2\text{ZnSnSe}_4$ and stannite $\text{Cu}_2\text{ZnSnSe}_4$ belonging to space groups $I\bar{4}$ (No. 82) and $I\bar{4}2m$ (No. 121) [31], respectively. Low symmetry can favorite the strengthening anharmonic vibration of phonon, and thus the low symmetry materials such as SnSe, Zn_4Sb_3 and MgAgSb usually possess low lattice thermal conductivity [32]. Furthermore, it is expected Ag_2XYSe_4 have high electrical conductivity due to containing two Ag atoms in each primitive unit cell. To the best of our knowledge, there have been no theoretical reports on the TE properties of Ag_2XYSe_4 (X=Ba, Sr; Y=Sn, Ge).

Hence, in this work, we used density functional theory (DFT) with semi-classical Boltzmann equation to explore the TE properties of p- and n-type Ag_2XYSe_4 (X=Ba, Sr; Y=Sn, Ge). It is showed that band gaps of $\text{Ag}_2\text{BaGeSe}_4$, $\text{Ag}_2\text{BaSnSe}_4$, $\text{Ag}_2\text{SrGeSe}_4$ and $\text{Ag}_2\text{SrSnSe}_4$ are 0.909 eV, 0.832 eV, 0.708 eV and 0.729 eV, being good for electrical transport properties. In addition, their lattice thermal conductivities are $2.22 \text{ Wm}^{-1}\text{K}^{-1}$, $1.95 \text{ Wm}^{-1}\text{K}^{-1}$, $2.26 \text{ Wm}^{-1}\text{K}^{-1}$ and $2.00 \text{ Wm}^{-1}\text{K}^{-1}$ at 300 K that are obviously lower than $3.2 \text{ Wm}^{-1}\text{K}^{-1}$ of $\text{Cu}_2\text{ZnSnSe}_4$ [27]. Lattice thermal conductivity at high temperature for each compound is below $1.0 \text{ Wm}^{-1}\text{K}^{-1}$. It is predicted that the n-type $\text{Ag}_2\text{SrGeSe}_4$ is the most excellent in the compounds Ag_2XYSe_4 (X=Ba, Sr; Y=Sn, Ge), having maximum ZT value of 1.15 (at 900K), and its p-type counterpart has a ZT value of 1.01. The ZT of both p-type $\text{Ag}_2\text{BaSnSe}_4$ and $\text{Ag}_2\text{SrSnSe}_4$ are above unity. This paper reveals Ag_2XYSe_4 is a new family of promising candidates for TE materials and may pave a way for seeking TE materials with high the ZT values.

We organize the rest of this paper as follows: the detailed computational method and some important parameters for first-principles calculations are presented in Sec. II.

The electronic structures, mechanical and thermal and thermoelectric properties are described and discussed in Sec. III. Finally, findings and conclusions are summarized in Sec. IV.

II. THEORETICAL CALCULATION DETAILS

Firstly, structure optimizations were performed using the generalized gradient approximation of Perdew, Burke, and Ernzerhof (GGA-PBE)[33] as the electronic exchange-correlation functional in VASP code. The plane-wave energy cutoff and Monckhorst-Pack k -point mesh were set to 500 eV and $10 \times 10 \times 10$, and the total-energy and force convergences were 10^{-6} eV and 10^{-3} eV/Å.

Secondly, we used the full potential method with GGA-PBE modified Becke and Johnson potential scheme (mBJ) [34] to calculate electronic structures for all compounds in Wien2k code [35]. In the whole calculation procedure, the total-energy and charge convergences were taken as 0.0001 eV and 0.0001 e . 3000 k -points in the whole first Brillouin Zone were sampled for calculations such as band structures and density of states. Taking a very dense 20000 k -points, the electrical transport parameters such as the Seebeck coefficient, the electrical conductivity and electronic thermal conductivity, were calculated using the semi-classical Boltzmann theory. In this theoretical framework, the electrical transport parameters can be described as follows [36]:

$$\sigma_{\alpha\beta}(T, E_F) = \frac{1}{\Omega} \int \sigma_{\alpha\beta}(\varepsilon) \left[-\frac{\partial f}{\partial \varepsilon} \right] d\varepsilon, \quad (1)$$

$$S_{\alpha\beta}(T, E_F) = (\sigma^{-1})_{i\alpha} \eta_{i\beta}, \quad (2)$$

$$\kappa_{\alpha\beta}(T, E_F) = \kappa_{\alpha\beta}^0 - T \eta_{\alpha m} (\sigma^{-1})_{nm} \eta_{m\beta}, \quad (3)$$

where T , E_f , Ω , f and ε are the absolute temperature, Fermi energy, unit cell volume, Fermi-Dirac distribution function and energy for electronic state. The energy projected conductivity tensors, $\sigma_{\alpha\beta}$, can be expressed as the following form

$$\sigma_{\alpha\beta}(\varepsilon) = \frac{e^2 \tau}{N} \sum_{i,k} v_{\alpha} v_{\beta} \frac{\delta(\varepsilon - \varepsilon_{i,k})}{d\varepsilon}, \quad (4)$$

herein, e is the charge of an electron, τ is the carrier relaxation time, N is the total number of sampled \mathbf{k} -points, $\varepsilon_{i,k}$ is the energy for the k th point at the i th band structure. The other physical parameters are given as follows

$$\eta_{\alpha\beta}(T, E_f) = \frac{1}{eT\Omega} \int \sigma_{\alpha\beta}(\varepsilon)(\varepsilon - E_f) \left[-\frac{\partial f}{\partial \varepsilon} \right] d\varepsilon, \quad (5)$$

$$\kappa_{\alpha\beta}^0(T, E_f) = \frac{1}{e^2T\Omega} \int \sigma_{\alpha\beta}(\varepsilon)(\varepsilon - E_f)^2 \left[-\frac{\partial f}{\partial \varepsilon} \right] d\varepsilon. \quad (6)$$

Note, $\kappa_{\alpha\beta}$ is the electronic thermal conductivity without the external electric field. It is well known that the precise calculation for the carrier relaxation time is difficult to be implemented due to complex carrier-scattering mechanism. In this paper, we mainly considered the carrier-photon scattering using the Fermi-golden rule combined with the deformation potential (DP) theory. According to the Fermi-golden rule, the scattering rate P_k at the electronic state \mathbf{k} can be described by

$$P_{kk'} = \sum_{k'} |M(\mathbf{k}, \mathbf{k}')|^2 \delta[\varepsilon(\mathbf{k}) - \varepsilon(\mathbf{k}') \pm \Delta E], \quad (7)$$

where the matrix element $M(\mathbf{k}, \mathbf{k}')$ represents the scattering from \mathbf{k} state to \mathbf{k}' state, which is known as the transition matrix element, ΔE is the phonon energy. In this work, we taken the phonon energy as $3k_B T$. Based on solid state physics theory, the reciprocal of the carrier relaxation time can expressed as:

$$\frac{1}{\tau(\mathbf{k})} = \sum_{k'} P_{kk'} (1 - \cos \theta) = \sum_{k'} |M(\mathbf{k}, \mathbf{k}')|^2 \delta[\varepsilon(\mathbf{k}) - \varepsilon(\mathbf{k}') \pm \Delta E] (1 - \cos \theta). \quad (8)$$

Herein, the angle θ is between the \mathbf{k} state to the \mathbf{k}' state. In the scattering process, the carrier absorbs or emits a phonon. Thus, by the DP theory, the effective transition matrix element around the valence band maximum (VBM) or conduction band maximum (CBM) can be given by [37]

$$|M|^2 = \frac{k_B T E_\beta^2}{\Omega c_\beta}, \quad (9)$$

where E_β and c_β are the deformation potential constant and elastic constant along the β direction. It is noted that the anisotropy is neglected and the matrix element M is independent of the θ in the DP theory, and thus the above equation can be described as

$$\frac{1}{\tau(\mathbf{k})} = \sum_{k'} |M(\mathbf{k}, \mathbf{k}')|^2 \delta[\varepsilon(\mathbf{k}) - \varepsilon(\mathbf{k}') \pm \Delta E], \quad (10)$$

it is worth noticing that the anisotropy is not completely ignored, and arises from the

anisotropic deformation potential constants and anisotropic elastic constants, which has small difference in the different directions.

Subsequently, we used slack's equation (see Eq. 11) to calculate the lattice thermal conductivities for all systems [38].

$$\kappa_L = A \frac{\Theta_D^3 V_{per}^{1/3} \bar{m}}{\gamma_a^2 n_{tot}^{2/3} T}. \quad (11)$$

Herein, A is a collection of physical constants with the value of about 3.04×10^{-6} , Θ_D is the Debye temperature, V_{per} is the volume per atom, \bar{m} is the average atom mass in the whole unit cell, n_{tot} is the total number of all atoms in the primitive unit cell. γ_a is the Grüneisen parameter for only acoustic phonons, which can be determined by [39]

$$\gamma_a = \frac{9v_l^2 - 12v_t^2}{2v_l^2 + 4v_t^2}, \quad (12)$$

where v_l and v_s are the velocities of longitudinal and transverse waves, which can be described by the bulk modulus B and the shear modulus G [40]

$$v_s = \left(\frac{3B + 4G}{3\rho} \right)^{1/2}, \quad v_p = \left(\frac{G}{\rho} \right)^{1/2}. \quad (13)$$

The Debye temperature Θ_D mentioned above is calculated by

$$\Theta_D = \frac{h}{k_B} \left(\frac{3n_{tot} N_A \rho}{4\pi M} \right)^{1/3} v_m, \quad (14)$$

$$v_m = \left[\frac{1}{3} \left(\frac{2}{v_s^3} + \frac{1}{v_p^3} \right) \right]^{-1/3}, \quad (15)$$

where physical constants h , N_A are the Plank's constant and Avogadro's number, M and ρ are the total atomic mass in primitive unit cell and the volume density of materials, v_m is the average sound velocity given by the velocities for transverse and longitude waves velocities v_l and v_s . We describe the details for the computation in earlier works [41-44].

III. RESULTS AND DISCUSSION

A Crystal and electronic structures

As is known, previous experimental and theoretical works have verified that the four compounds Ag_2XYSe_4 possess the orthorhombic crystal structures with space group $I222$ (No. 23) that has lower symmetry than $\text{Cu}_2\text{ZnSnQ}_4$ ($Q=\text{S, Se}$). It is expected that Ag_2XYSe_4 have lower thermal conductivities than $\text{Cu}_2\text{ZnSnQ}_4$. Experimental

structure determinations for $\text{Ag}_2\text{BaSnSe}_4$ and $\text{Ag}_2\text{BaGeSe}_4$ have been reported, and lattice constants for the other two compounds are theoretically predicted, also. These data are summarized in Table I. The optimized lattice constants in this work are in agreement with the experimental data [29,45] and the largest difference is less than 3.5%. For the other two compounds, our theoretical lattice constants and other theoretical data predicted by HSE06 hybrid DFT calculations [30] are very consistent with each other, and the largest differences is less than 1.5%.

TABLE I. Experimental and calculated lattice constants (in Å) and calculated band gaps (in eV) of Ag_2XYSe_4 (X=Ba, Sr; Y=Sn, Ge) using different exchange-correlation functionals (PBE, mBJ and HSE06).

	$\text{Ag}_2\text{BaGeSe}_4$		$\text{Ag}_2\text{BaSnSe}_4$		$\text{Ag}_2\text{SrGeSe}_4$		$\text{Ag}_2\text{SrSnSe}_4$	
	This work	Expt. ^a	This work	Expt. ^b	This work	Theo. ^c	This work	Theo. ^c
a (Å)	7.053	7.058	7.141	7.116	7.110	7.115	7.183	7.193
b (Å)	7.501	7.263	7.713	7.499	7.413	7.389	7.673	7.657
c (Å)	8.481	8.263	8.582	8.337	8.061	7.951	8.135	8.034
PBE Bandgap (eV)	0.284		0.195		0.000		0.041	
mBJ Bandgap (eV)	0.909		0.832		0.708		0.729	
HSE06 Bandgap (eV) ^c	0.85		0.77		0.68		0.66	

^a From Ref. [29]

^b From Ref. [45]

^c From Ref. [30]

We took theoretical lattice constants in this work for the self-consistent calculations and then calculated the band structures along the high-symmetry points showed in Fig. 1(a0 and a-d). There are three obvious localized valence band maximums (VBMs) and a few localized conduction band minimums (CBMs) in each compound. Valence bandwidth (VBW) for each compound is about 2 eV greater than its conduction bandwidth (CBW) of about 0.5 eV. This implies that the n-type carriers have larger effective mass than that for the p-type. Note that $\text{Ag}_2(\text{Ba}/\text{Sr})\text{SnSe}_4$ have narrower VBW than $\text{Ag}_2(\text{Ba}/\text{Sr})\text{GeSe}_4$ because the Se-Sn hybridizations that constitute the main

components of the conduction bands, are weaker than the Ge-Se hybridizations showed in Fig. 1(e)-(h). The Se-Ag hybridizations are the major ingredient of valence bands in all the compounds, implying strong Se-Ag covalent bonds in bulk materials. The Ba/Sr atoms have negligible contributions to the density of states (DOS) in the energy range from -3 eV to 4 eV. It is expected that doping the vacancies or heterogeneous atoms at the sites of Ba/Sr atoms can result in lower lattice thermal conductivity with little effect on electronic transport properties. The PBE, mBJ and HSE06-hybrid (in Ref. [30]) band gaps for the four compounds are also listed in Table I. The mBJ band gaps are obviously bigger than the PBE and HSE06-hybrid band gaps. It is worth mentioning that the normal PBE method usually underestimates the band gaps, but the mBJ method, comparable with GW, usually get band gaps in good agreement with the experimental data. $\text{Ag}_2\text{BaGeSe}_4$ has the largest band gap of 0.909 eV in four compounds and $\text{Ag}_2\text{SrGeSe}_4$ has the smallest band gap of 0.708 eV, which are close to the band gap 0.86 eV for the state-of-the-art TE material SnSe.

In order to further study on electronic structures, taking $\text{Ag}_2\text{BaGeSe}_4$ as an example, its p- and n-type Fermi surfaces are presented in Fig. 2. It is seen that there are six ellipsoidal hole pockets and six spherical electron pockets. Half of the pockets appears near high symmetry points Y, X-L and X1-Z in good agreement with band structures. The remaining half pockets appear near the equivalence sites of these high symmetric points. Good TE materials usually have many electron or hole pockets. For instance, n-type CoSb_3 and PbTe have 12 and 4 pockets respectively [22,46], p- and n-type high-temperature phase SnSe have 4 and 3 pockets [47]. From the electronic structure, band gaps and carrier pockets are two intuitive parameters to assess the thermoelectric properties of materials. Comparing Ag_2XYSe_4 (X=Ba, Sr; Y=Sn, Ge) with SnSe, they have at least two similarities: suitable band gaps 0.7 eV~1.0 eV and multiple carrier pockets. The band gaps are not too big or too small, which not only keep away from bipolar effect but also are good for achieving high Seebeck coefficient. Multiple carrier pockets not only provide more carrier to participate in the conduction, but also support the possibility of light and heavy band coexisting near the Fermi level. The heavy band introduces the carriers with high Seebeck coefficient, the opposite relationship between

electrical conductivity and Seebeck coefficient can be alleviated. Thus, it is of great possibility to realize high ZT for Ag_2XYSe_4 by regulating carrier density and other technical means.

B Mechanical and thermal properties

In this section, we put focus on mechanical and thermal properties. Calculated elastic constants, bulk and shear moduli, velocities of transverse and longitudinal waves, Poisson's ratios, Debye temperatures and acoustic Grüneisen parameters for four compounds are listed in Table II. There are nine independent elastic constants (c_{11} , c_{22} , c_{33} , c_{44} , c_{55} , c_{66} , c_{12} , c_{13} and c_{23}) for an orthogonal crystal. The values of elastic constants with the same subscript for different compounds are very close. However, for one material, it is found that elastic constants c_{11} , c_{22} and c_{33} along the major directions are larger than the other. The c_{11} is the largest, c_{33} is the smallest in c_{11} , c_{22} and c_{33} . Correspondingly, lattice constants a and c are the shortest and longest. It is understandable that short lattice constant indicates strong interactions between atoms along the axis, which inevitably cause large elastic constant. Besides, the elastic constants can be used to measure structural mechanical stability. The criteria of mechanical stability for orthogonal crystals are expressed by [48]

$$c_{11} > 0, c_{22} > 0, c_{33} > 0, c_{44} > 0, c_{55} > 0, c_{66} > 0, \quad (16)$$

$$c_{11} + c_{22} + c_{33} + 2c_{12} + 2c_{13} + 2c_{23} > 0, \quad (17)$$

$$c_{11} + c_{22} - 2c_{12} > 0, \quad (18)$$

$$c_{11} + c_{13} - 2c_{13} > 0, \quad (19)$$

$$c_{22} + c_{33} - 2c_{23} > 0. \quad (20)$$

It is clear that four compounds are of mechanical stability. The calculated bulk moduli B are larger than the calculated shear modulus G , which implies that they have good machinability and thus are not fragile. In macroscopic view, Poisson's ratio can estimate the corresponding lateral strain to applied axial strain. Microcosmically, it represents the degree of covalent bond. The small value of Poisson's ratio is indicative of covalent bond, the large value represents strong ionic or metallic bonds [49]. For pure silver and selenium bulks, Poisson's ratios are about 0.367 and 0.447 [50] that are larger than about 0.3 for Ag_2XYSe_4 . This indicates that there are covalent bonds in four compounds,

which is agreeing with results from electronic band structures. It is noted that the coexisting of many types of bonds are beneficial to the improvement of thermoelectric performance [51]. Metal bonds represent high electronic conductivity, ionic bonds usually is along with high Seebeck coefficient.

TABLE II. Calculated elastic constants c_{ij} in GPa, bulk and shear moduli B and G in GPa, velocities of transverse and longitudinal waves v_t and v_l in m/s , Poisson's ratios ν , Debye temperatures Θ in K and acoustic Grüneisen parameters γ_a for Ag_2XYSe_4 (X=Ba, Sr; Y=Sn, Ge).

	$\text{Ag}_2\text{BaGeSe}_4$	$\text{Ag}_2\text{BaSnSe}_4$	$\text{Ag}_2\text{SrGeSe}_4$	$\text{Ag}_2\text{SrSnSe}_4$
c_{11}	90.1953	90.8454	98.4429	99.8721
c_{22}	56.0873	64.6186	66.9605	63.6739
c_{33}	52.2170	52.8386	62.3014	56.6002
c_{44}	24.5931	22.7369	24.7166	23.2939
c_{55}	26.0964	21.4068	25.2265	23.4543
c_{66}	33.7824	31.6366	29.2304	30.8721
c_{12}	48.8688	53.5752	54.4242	56.4909
c_{13}	33.0205	29.9881	35.1455	32.7599
c_{23}	9.3571	30.3142	29.9960	30.7913
B	44.207	45.954	49.460	48.150
G	20.685	19.939	21.969	20.606
v_t	1944.30	1900.12	2016.75	1943.25
v_l	3622.08	3624.24	3818.37	3722.74
v_a	2171.08	2125.24	2254.55	2174.10
ν	0.297	0.310	0.306	0.312
Θ	212.535	204.537	224.897	212.985
γ_a	1.75	1.83	1.81	1.85

Other two important thermal parameters Θ and γ_a are listed TABLE II, also. The Debye temperatures for four compounds are all below 230 K, and $\text{Ag}_2\text{BaSnSe}_4$ has the lowest Θ of 204 K. The acoustic Grüneisen parameter γ_a for each compound is above 1.70, and $\text{Ag}_2\text{SrSnSe}_4$ have largest γ_a of 1.85. According to Eq. (11), low Θ and high γ_a can lead to low lattice conductivity. Low Θ indicates weak forces between atoms and atoms in the crystal, which is usually along with high γ_a . The high γ_a represent strong anharmonic vibrations, favorable for obtaining a low κ_L . However, note that low Θ and

high γ_a bring a drawback: low melting point. This is what we need to pay attention to solving in practical application. Furthermore, it is worth pointing out that γ_a only contains acoustic wave components, which is usually have a large difference from the mode averaged Gruneisen parameter.

C Thermoelectric properties

The carrier relaxation time τ is very important physical parameter for calculations of electrical conductivity and electronic thermal conductivity. In this work, only the interaction between acoustic phonon and carrier, is taken into account in calculation of the carrier relaxation time showed in Fig. 3. It is found that τ for each compound lowers with increasing T and is of the order of magnitude of 10^{-14} to 10^{-15} . τ for p-type $\text{Ag}_2\text{BaSnSe}_4$, $\text{Ag}_2\text{SrGeSe}_4$ and $\text{Ag}_2\text{SrSnSe}_4$ is larger than their n-type. However, τ for p-type $\text{Ag}_2\text{BaGeSe}_4$ is smaller than that for its n-type below about 500 K.

TABLE III. Calculated Seebeck coefficients S in μVK^{-1} , electrical conductivities σ in 10^5Sm^{-1} , lattice thermal conductivities κ_L in $\text{Wm}^{-1}\text{K}^{-1}$, optimal carrier densities n in 10^{19}cm^{-3} and figure of merit ZT for p- and n-type Ag_2XYSe_4 ($X=\text{Ba}, \text{Sr}$; $Y=\text{Sn}, \text{Ge}$) at 300 K.

	p-type					n-type				
	S	σ	κ_L	n	ZT	S	σ	κ_L	n	ZT
$\text{Ag}_2\text{BaGeSe}_4$	142	0.62	2.22	3.02	0.14	-158	0.93	2.22	3.02	0.25
$\text{Ag}_2\text{BaSnSe}_4$	170	0.55	1.95	1.90	0.21	-152	0.75	1.95	7.58	0.21
$\text{Ag}_2\text{SrGeSe}_4$	169	0.64	2.26	1.73	0.20	-173	0.56	2.26	2.08	0.19
$\text{Ag}_2\text{SrSnSe}_4$	171	0.56	2.00	1.90	0.21	-149	1.04	2.00	4.36	0.25

The ZT with respect to T and n in a sufficiently broad region (n, T) are plotted in Fig. 4. The large ZT are concentrated in high T and large n region, and the large ZT for both n-type $\text{Ag}_2\text{BaSnSe}_4$ and $\text{Ag}_2\text{SrSnSe}_4$ form closed regions. The maximum ZT for p- and n-type $\text{Ag}_2\text{BaGeSe}_4$ is below unity, but p- and n-type $\text{Ag}_2\text{SrGeSe}_4$ have

maximum ZT up to 1.01 and 1.15, respectively. The maximum ZT for the p-type $\text{Ag}_2\text{BaSnSe}_4$ and $\text{Ag}_2\text{SrSnSe}_4$ are both larger than unity and the maximum ZT for n-type are smaller than unit. It is found that the maximum ZT for n-type $\text{Ag}_2\text{BaSnSe}_4$ and $\text{Ag}_2\text{SrSnSe}_4$ appear at ~ 670 K and ~ 810 K, all the other appear at 900 K.

In order to study TE properties in detail, we summarized the Seebeck coefficients, electrical conductivities, lattice thermal conductivities and figure of merits with fixed optimal carrier densities at 300 K and 900 K in Tables III and IV, and the corresponding values for these parameters at 600K are listed in Table SII of the Supplementary Material. Absolute Seebeck coefficient $|S|$ for each compound at 300 K are above $100 \mu\text{VK}^{-1}$ and below $200 \mu\text{V K}^{-1}$, and electrical conductivities for p- and n-type are all below $1 \times 10^5 \text{ Sm}^{-1}$ except the n-type $\text{Ag}_2\text{SrSnSe}_4$ with the σ that is up to $1.04 \times 10^5 \text{ Sm}^{-1}$. When temperature increases from 300 K to 900 K, the electrical conductivities for most of compounds decrease but p-type $\text{Ag}_2\text{BaGeS}_4$ is on the contrary, and absolute Seebeck coefficients for most of compounds except p- and n-type $\text{Ag}_2\text{BaGeS}_4$ increase. Absolute Seebeck coefficients for n-type $\text{Ag}_2\text{SrGeSe}_4$ can reach up to $245 \mu\text{VK}^{-1}$.

TABLE IV. Calculated Seebeck coefficients S in μVK^{-1} , electrical conductivities σ in 10^5Sm^{-1} , lattice thermal conductivities κ_L in $\text{Wm}^{-1}\text{K}^{-1}$, optimal carrier densities n in 10^{19}cm^{-3} and figure of merit ZT for p- and n-type Ag_2XYSe_4 (X=Ba, Sr; Y=Sn, Ge) at 900 K.

	p-type					n-type				
	S	σ	κ_L	n	ZT	S	σ	κ_L	n	ZT
$\text{Ag}_2\text{BaGeSe}_4$	112	0.81	0.74	19.05	0.35	-138	0.89	0.74	33.11	0.62
$\text{Ag}_2\text{BaSnSe}_4$	240	0.19	0.65	4.36	1.03	-197	0.07	0.65	39.81	0.38
$\text{Ag}_2\text{SrGeSe}_4$	237	0.22	0.75	3.98	1.01	-245	0.25	0.75	8.31	1.15
$\text{Ag}_2\text{SrSnSe}_4$	239	0.20	0.66	4.36	1.04	-200	0.16	0.66	36.30	0.72

The calculated lattice thermal conductivities at 300 K for all compounds are about

$2 \text{ Wm}^{-1}\text{K}^{-1}$ which are lower than $\sim 3.2 \text{ Wm}^{-1}\text{K}^{-1}$ of $\text{Cu}_2\text{ZnSnSe}_4$, and are decreasing with increasing temperature. All calculated lattice thermal conductivities at 900 K are below $1.0 \text{ Wm}^{-1}\text{K}^{-1}$, for example, $0.65 \text{ Wm}^{-1}\text{K}^{-1}$ for $\text{Ag}_2\text{BaSnSe}_4$. It is worth noting that the calculated lattice thermal conductivity should be higher than the actual thermal conductivity because optical wave scattering is neglected in Slack's equation. The optimal carrier densities at 300 K, 600 K and 900 K for the p-type are around 10^{19} cm^{-3} but that at 900 K for p-type $\text{Ag}_2\text{BaGeS}_4$ is up to $1.905 \times 10^{20} \text{ cm}^{-3}$. The optimal carrier densities at 300 K for the n-type are around 10^{19} cm^{-3} also, but most of those at 600 K and 900 K are around 10^{20} cm^{-3} . These optimal carrier densities can be well approached by doping or non-stoichiometry means.

IV. CONCLUSIONS

In summary, we use the first-principles method with mBJ scheme to systematically explore electronic structures, mechanical and thermal and TE properties of p- and n-type Ag_2XYSe_4 (X=Ba, Sr; Y=Sn, Ge). It is found that low crystal symmetry, and suitable band gap and several carrier pockets mainly contribute to weak thermal transport property and medium electrical transport performance. It is predicted that the largest ZT in the p-type Ag_2XYSe_4 comes from $\text{Ag}_2\text{SrSnSe}_4$ compound reaching up to 1.04 at 900 K, and the largest ZT in the n-type is 1.15 of $\text{Ag}_2\text{SrGeSe}_4$ at 900 K. Although the values for ZT is not very excellent, we believe the ZT for those compounds do be prompted by such as doping, low-dimensional strategy. In a word, Ag_2XYSe_4 (X=Ba, Sr; Y=Sn, Ge) are a kind of potential TE materials.

ACKNOWLEDGMENTS

Authors gratefully acknowledge great support from the National Natural Science Foundation of China (Grant No. 11804132).

- [1] M. Meinero, F. Caglieris, G. Lamura, I. Pallecchi, A. Jost, U. Zeitler, S. Ishida, H. Eisaki, and M. Putti, *Phys. Rev. B* **98**, 155116 (2018).
- [2] L. D. Zhao *et al.*, *Science* **351**, 141 (2016).
- [3] J. Mao, Z. H. Liu, and Z. F. Ren, *Npj Quantum Materials* **1**, 16028 (2016).
- [4] J. Z. Xin, Y. L. Tang, Y. T. Liu, X. B. Zhao, H. G. Pan, and T. J. Zhu, *Npj Quantum Materials* **3**, 9 (2018).
- [5] L. D. Zhao, S. H. Lo, Y. S. Zhang, H. Sun, G. J. Tan, C. Uher, C. Wolverton, V. P. Dravid, and M. G. Kanatzidis, *Nature* **508**, 373 (2014).
- [6] C. G. Fu, T. J. Zhu, Y. Z. Pei, H. H. Xie, H. Wang, G. J. Snyder, Y. Liu, Y. T. Liu, and X. B. Zhao, *Advanced Energy Materials* **4**, 1400600 (2014).
- [7] Q. Y. Zhang *et al.*, *Energy Environ. Sci.* **5**, 5246 (2012).
- [8] Y. Z. Pei, H. Wang, and G. J. Snyder, *Adv. Mater.* **24**, 6125 (2012).
- [9] W. S. Liu, X. Yan, G. Chen, and Z. F. Ren, *Nano Energy* **1**, 42 (2012).
- [10] E. Quarez, K. F. Hsu, R. Pcionek, N. Frangis, E. K. Polychroniadis, and M. G. Kanatzidis, *J. Am. Chem. Soc.* **127**, 9177 (2005).
- [11] H. Kamila, P. Sahu, A. Sankhla, M. Yasseri, H. N. Pham, T. Dasgupta, E. Mueller, and J. de Boor, *J. Mater. Chem. A* **7**, 1045 (2019).
- [12] Y. Z. Pei, A. F. May, and G. J. Snyder, *Advanced Energy Materials* **1**, 291 (2011).
- [13] F. S. Kim, K. Suekuni, H. Nishiata, M. Ohta, H. I. Tanaka, and T. Takabatake, *J. Appl. Phys.* **119**, 175105 (2016).
- [14] W. Wang, M. T. Winkler, O. Gunawan, T. Gokmen, T. K. Todorov, Y. Zhu, and D. B. Mitzi, *Advanced Energy Materials* **4**, 175105 (2014).
- [15] S. Ahn, S. Jung, J. Gwak, A. Cho, K. Shin, K. Yoon, D. Park, H. Cheong, and J. H. Yun, *Appl. Phys. Lett.* **97**, 021905 (2010).
- [16] F. Luckert *et al.*, *Appl. Phys. Lett.* **99**, 062104 (2011).
- [17] S. G. Choi, T. J. Kim, S. Y. Hwang, J. Li, C. Persson, Y. D. Kim, S. H. Wei, and I. L. Repins, *Sol. Energ. Mat. Sol. C.* **130**, 375 (2014).
- [18] S. G. Choi, H. Y. Zhao, C. Persson, C. L. Perkins, A. L. Donohue, B. To, A. G. Norman, J. Li, and I. L. Repins, *J. Appl. Phys.* **111**, 033506 (2012).
- [19] S. Y. Chen, A. Walsh, X. G. Gong, and S. H. Wei, *Adv. Mater.* **25**, 1522 (2013).
- [20] M. Salavati-Niasari, M. Bazarganipour, and F. Davar, *J. Alloy. Compd.* **489**, 530 (2010).
- [21] A. Svane, N. E. Christensen, M. Cardona, A. N. Chantis, M. van Schilfgaarde, and T. Kotani, *Phys. Rev. B* **81**, 245120 (2010).
- [22] Y. L. Tang, Z. M. Gibbs, L. A. Agapito, G. Li, H. S. Kim, M. B. Nardelli, S. Curtarolo, and G. J. Snyder, *Nat. Mater.* **14**, 1223 (2015).
- [23] R. Hea *et al.*, *Proceedings of the National Academy of Sciences of the United States of America* **113**, 13576 (2016).
- [24] J. Soga, T. Iida, Y. Higuchi, T. Sakuma, K. Makino, M. Akasaka, T. Nemoto, and Y. Takanashi, *ICT: 2005 24th International Conference on Thermoelectrics*, 95 (2005).
- [25] I. H. Kim, *J. Korean Phys. Soc.* **72**, 1095 (2018).
- [26] N. Savvides and H. Y. Chen, *J. Electron. Mater.* **39**, 2136 (2010).
- [27] X. Y. Shi, F. Q. Huang, M. L. Liu, and L. D. Chen, *Appl. Phys. Lett.* **94**, 122103 (2009).
- [28] M. L. Liu, I. W. Chen, F. Q. Huang, and L. D. Chen, *Adv. Mater.* **21**, 3808 (2009).

- [29] M. Tampier and D. Johrendt, *Z. Anorg. Allg. Chem.* **627**, 312 (2001).
- [30] T. Zhu, W. P. Huhn, G. C. Wessler, D. Shin, B. Saparov, D. B. Mitzi, and V. Blum, *Chem. Mater.* **29**, 7868 (2017).
- [31] S. Y. Chen, X. G. Gong, A. Walsh, and S. H. Wei, *Appl. Phys. Lett.* **94**, 041903 (2009).
- [32] J. Li *et al.*, *Joule* **2**, 976 (2018).
- [33] J. P. Perdew, K. Burke, and M. Ernzerhof, *Phys. Rev. Lett.* **77**, 3865 (1996).
- [34] F. Tran and P. Blaha, *Phys. Rev. Lett.* **102**, 226401 (2009).
- [35] K. Schwarz, P. Blaha, and G. K. H. Madsen, *Comput. Phys. Commun.* **147**, 71 (2002).
- [36] G. K. H. Madsen and D. J. Singh, *Comput. Phys. Commun.* **175**, 67 (2006).
- [37] J. Bardeen and W. Shockley, *Physical Review* **80**, 72 (1950).
- [38] G. A. Slack, *J. Phys. Chem. Solids* **34**, 321 (1973).
- [39] B. D. Sanditov, S. B. Tsydypov, and D. S. Sanditov, *Acoust. Phys+* **53**, 594 (2007).
- [40] J. Feng, C. L. Wan, B. Xiao, R. Zhou, W. Pan, and D. R. Clarke, *Phys. Rev. B* **84**, 024302 (2011).
- [41] Y. Liu, D. Z. Zhou, Y. Q. Li, A. J. Hong, J. H. Sui, J. M. Liu, and Z. F. Ren, *J. Mater. Chem. A* **6**, 2600 (2018).
- [42] A. J. Hong, C. L. Yuan, G. Gu, and J. M. Liu, *J. Mater. Chem. A* **5**, 9785 (2017).
- [43] A. J. Hong, L. Li, R. He, J. J. Gong, Z. B. Yan, K. F. Wang, J. M. Liu, and Z. F. Ren, *Sci. Rep.* **6**, 22778 (2016).
- [44] A. J. Hong, J. J. Gong, L. Li, Z. B. Yan, Z. F. Ren, and J. M. Liu, *J. Mater. Chem. C* **4**, 3281 (2016).
- [45] A. Assoud, N. Soheilnia, and H. Kleinke, *Chem. Mater.* **17**, 2255 (2005).
- [46] Y. Z. Pei, X. Y. Shi, A. LaLonde, H. Wang, L. D. Chen, and G. J. Snyder, *Nature* **473**, 66 (2011).
- [47] K. Kutorasinski, B. Wiendlocha, S. Kaprzyk, and J. Tobola, *Phys. Rev. B* **91**, 205201 (2015).
- [48] Z.-j. Wu, E.-j. Zhao, H.-p. Xiang, X.-f. Hao, X.-j. Liu, and J. Meng, *Phys. Rev. B* **76**, 054115 (2007).
- [49] Y. Pan, Y. Lin, Q. Xue, C. Ren, and H. Wang, *Mater. Design.* **89**, 676 (2016).
- [50] H. Gercek, *Int. J. Rock. Mech. Min.* **44**, 1 (2007).
- [51] A. J. Hong, L. Li, H. X. Zhu, Z. B. Yan, J. M. Liu, and Z. F. Ren, *J. Mater. Chem. A* **3**, 13365 (2015).

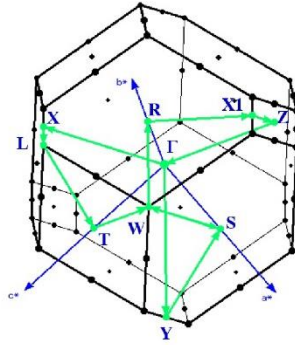
Figure Captions

FIG. 1. (Color online) Calculated band structures along high symmetry points (showed in (a0)) and DOS for Ag_2XYSe_4 ($\text{X}=\text{Ba}, \text{Sr}$; $\text{Y}=\text{Sn}, \text{Ge}$).

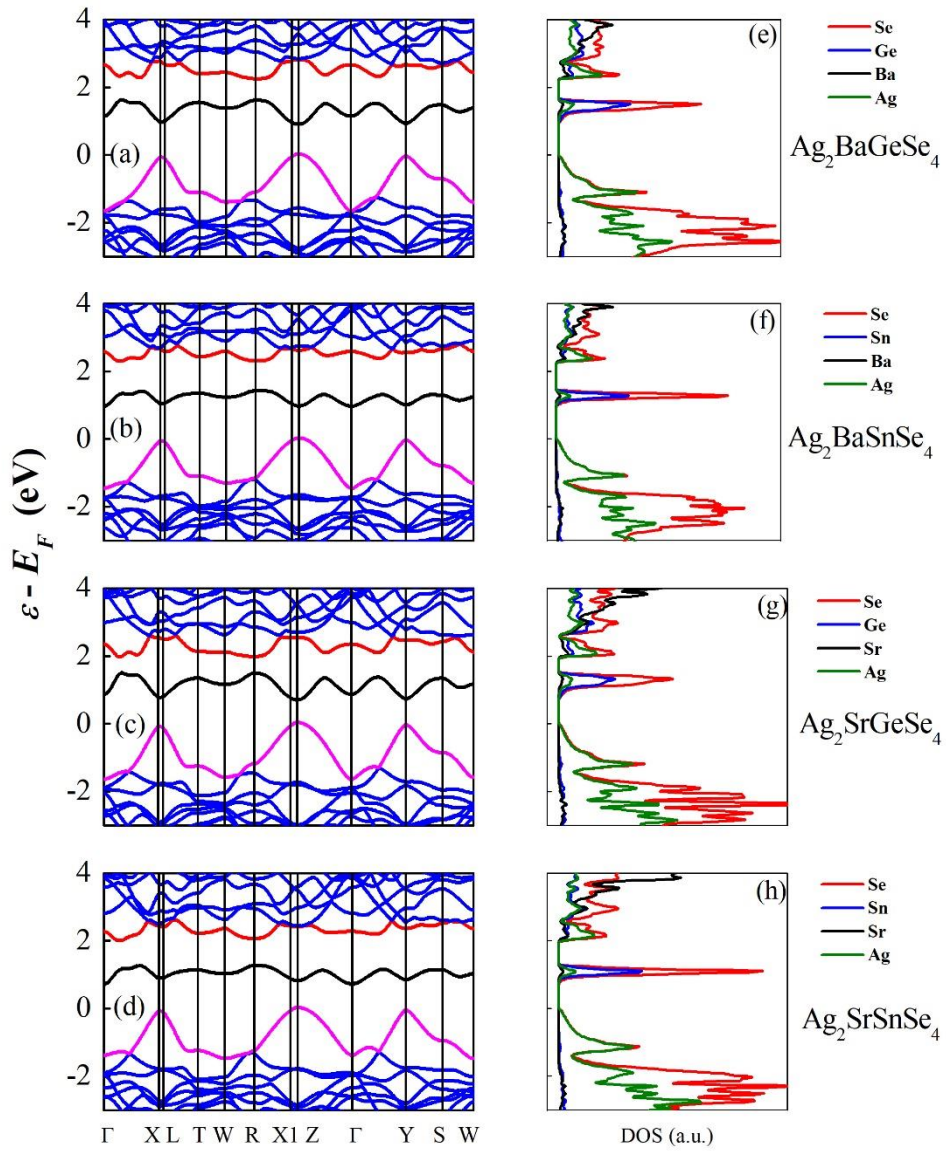
Fig. 2. (Color online) Fermi surfaces of p- and n-type $\text{Ag}_2\text{BaGeSe}_4$. Fermi levels are 0.015 Ry below the VBM for p-type and above the CBM for n-type.

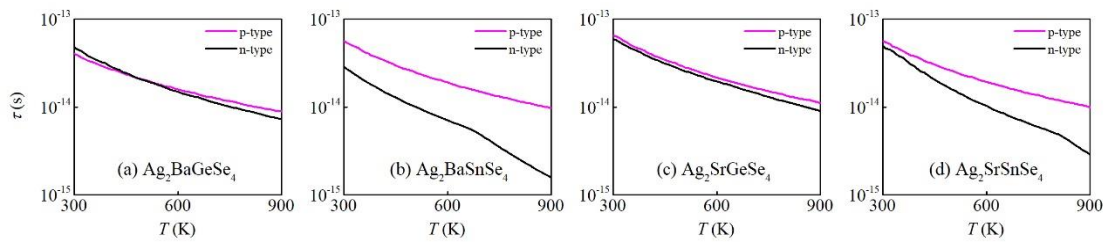
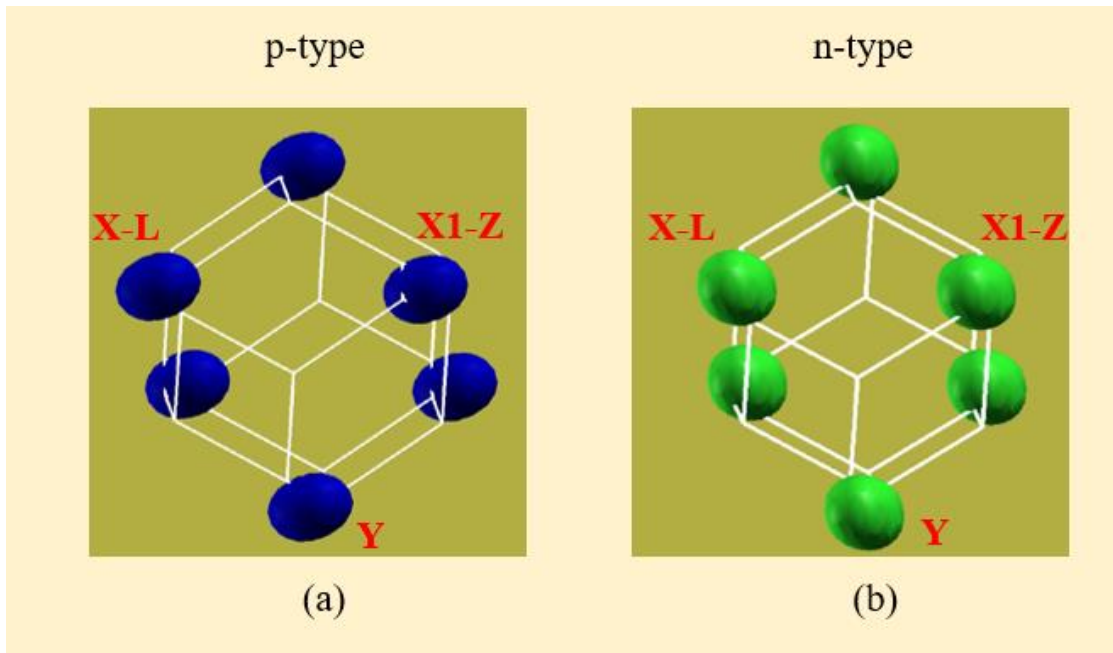
Fig. 3. (Color online) Calculated carrier relaxation time τ as a function of T for p- and n-type Ag_2XYSe_4 ($\text{X}=\text{Ba}, \text{Sr}$; $\text{Y}=\text{Sn}, \text{Ge}$).

FIG. 4. (Color online) Calculated ZT with respect to temperature T and carrier density n for p- and n-type Ag_2XYSe_4 ($\text{X}=\text{Ba}, \text{Sr}$; $\text{Y}=\text{Sn}, \text{Ge}$).



(a0)





p-type

n-type

